

**Electronic Supplementary Information:  
Heteronuclear DNP of  $^1\text{H}$  and  $^{19}\text{F}$  nuclei using BDPA as polarizing agent.**

Antonio Gennaro, Alexander Karabanov, Alexey Potapov\* and Walter Kckenberger  
School of Physics and Astronomy, University of Nottingham, University Park, Nottingham, NG7 2RD, UK  
\*corresponding author: alexey.potapov@nottingham.ac.uk

**CONTENTS**

ESR measurements	S2
Evolution of polarization in a system containing $^1\text{H}$ and $^{19}\text{F}$ nuclei	S2
Estimate of spectral diffusion effect in an inhomogeneous ESR line	S3
Additional Evidence for a Cross-Relaxation between $^1\text{H}$ and $^{19}\text{F}$ nuclei	S3
Minimal models of solid effect, heteronuclear thermal mixing and heteronuclear cross effect DNP	S7
Frame Transformation	S7
Average Hamiltonian for SE DNP	S8
Properties of the Spectral Densities $f_j(\lambda)$ and $f'_{kj}(\lambda)$	S10
Average Hamiltonian for hn-TM DNP	S11
Symmetry Breaking and Minimal Model	S11
The Heteronuclear Cross Effect	S12
Density Matrix Simulations	S13
References	S14

## ESR MEASUREMENTS

The ESR measurements were carried out using a home-built W-band pulse ESR spectrometer equipped with an Oxford Instruments superconducting magnet system where the main field is set at 3.4 T, and a sweepable magnet covers a range of  $\pm 0.1$  T. The variable temperature insert (VTI) allows cooling of the ESR sample. The VTI operates under continuous vacuum pumping and uses helium from the magnet reservoir for cooling the sample. The measurements were carried out at a temperature of  $\sim 30$  K. The design of the microwave (MW) bridge and the sample probe are very similar to the one reported by the Goldfarb group [1]. The pulses are generated using a DTG5078 data timing generator (Tektronix Inc.), video signals from the MW bridge are acquired using a TDS7154 oscilloscope (Tektronix Inc.), the magnetic field is controlled using a ISS-10 shim power supply, where one of the outputs is connected to the sweepable superconducting magnet. All these devices are controlled using a home written LabView program.

The field-sweep ESR spectra for  $[\text{BDPA}] = 1$  mM and  $[\text{BDPA}] = 40$  mM are shown in Fig.S1. The ESR line for  $[\text{BDPA}] = 1$  mM has a FWHH  $\approx 21$  MHz, which is dominated by the inhomogeneous broadening due to hyperfine couplings and  $g$ -anisotropy. For  $[\text{BDPA}] = 40$  mM the width is larger, FWHH  $\approx 27$  MHz, and has an additional contribution due to the dipolar couplings with many nearby electrons. The maxima of the two spectra shown in Fig.S1 do not coincide due to inaccuracy of field setting by the magnetic field controller.

## EVOLUTION OF POLARIZATION IN A SYSTEM CONTAINING $^1\text{H}$ AND $^{19}\text{F}$ NUCLEI

The Solomon equations describe the cross-relaxation in a system containing a pair of two spin-1/2 heteronuclei[2]. The magnetic moments of nuclei  $\hat{I}_z$  and  $\hat{S}_z$  can be found using the following relationships:

$$\begin{aligned} \frac{d\hat{I}_z}{dt} &= -(w_0 + 2w_1 + w_2) (\hat{I}_z - I_0) - \\ &\quad - (w_2 - w_0) (\hat{S}_z - S_0) \\ \frac{d\hat{S}_z}{dt} &= -(w_0 + 2w'_1 + w_2) (\hat{I}_z - I_0) - \\ &\quad - (w_2 - w_0) (\hat{I}_z - I_0) \end{aligned} \quad (1)$$

Here  $w_1$  and  $w'_1$  are the single quantum transition probabilities per unit time for spins  $\hat{I}$  and  $\hat{S}$  respectively,  $w_0$  is the zero quantum transition probability,  $w_2$  is the double-quantum transition probability per unit time, and  $S_0$  and  $I_0$  are the equilibrium values of the magnetic moments. The right-hand side of each equation is a *linear combination of magnetic moments*  $\hat{I}_z$  and  $\hat{S}_z$  with an additional constant. In our system, there are many  $^1\text{H}$  and

$^{19}\text{F}$ , with  $N_H$  – the number of  $^1\text{H}$  nuclei and  $N_F$  – the number of  $^{19}\text{F}$  nuclei, some of which cross-relax with one another, while the rest form a very dense network, such that polarization is quickly mixed among nuclei of same kind.

Taking into account the linearity of Solomon Eqs. (1), the solution for polarizations  $P_H(t)$  and  $P_F(t)$ , for  $^1\text{H}$  and  $^{19}\text{F}$  respectively, in such a sample should also be described by a *system of linear equations*:

$$\begin{aligned} \frac{dP_F(t)}{dt} &= a_1 P_H(t) + a_2 P_F(t) + a_3 \\ \frac{dP_H(t)}{dt} &= b_1 P_H(t) + b_2 P_F(t) + b_3 \end{aligned} \quad (2)$$

where  $a_1, a_2, a_3, b_1, b_2, b_3$  are some coefficients. The equations can be rewritten to give the coefficients some more physically meaningful form:

$$\begin{aligned} \frac{dP_F(t)}{dt} &= R_F [P_F(t) - P_{F,eq}] + \\ &\quad + \sigma_{H \rightarrow F} [P_F(t) - P_H(t)] \\ \frac{dP_H(t)}{dt} &= R_H [P_H(t) - P_{H,eq}] + \\ &\quad + \sigma_{F \rightarrow H} [P_F(t) - P_H(t)] \end{aligned} \quad (3)$$

Here  $R_F$  and  $R_H$  are the intrinsic relaxation rates of  $^{19}\text{F}$  and  $^1\text{H}$  nuclei,  $\sigma_{F \rightarrow H}$  and  $\sigma_{H \rightarrow F}$  are the rates of polarization transfer from  $^{19}\text{F}$  to  $^1\text{H}$  and reverse, respectively. Now, let us consider two scenarios for validating the equations:

- In the absence of cross-relaxation, i.e. when  $\sigma_{F \rightarrow H} = \sigma_{H \rightarrow F} = 0$ , both types of nuclei will exponentially relax with their respective rates  $R_F$  and  $R_H$  and polarizations will tend to their thermal equilibrium values,  $P_H(t \rightarrow \infty) \rightarrow P_{H,eq}$  and  $P_F(t \rightarrow \infty) \rightarrow P_{F,eq}$ .
- In the absence of intrinsic relaxation, i.e. when  $R_F = R_H = 0$ , the nuclei will only cross-relax. However, since only zero-quantum cross-relaxation is active, such cross-relaxation equalizes the polarizations over time, which is described by the second term in the left-hand side of Eqns.3. Furthermore, the cross-relaxation without intrinsic relaxation conserves the total spin angular momentum, such that

$$N_H P_H(t) + N_F P_F(t) = \text{const} \quad (4)$$

Combining Eqs. (3,4) gives:

$$\begin{aligned} \frac{d(N_H P_H(t) + N_F P_F(t))}{dt} &= \\ = (N_H \sigma_{F \rightarrow H} + N_F \sigma_{H \rightarrow F}) (P_F(t) - P_H(t)) &= 0 \end{aligned} \quad (5)$$

The expression equals zero at all times, only if  $N_F\sigma_{F\rightarrow H} + N_H\sigma_{H\rightarrow F} = 0$ , therefore  $\sigma_{H\rightarrow F} = -N_F/N_H\sigma_{F\rightarrow H}$ .

Finally, after renaming  $\sigma = \sigma_{H\rightarrow F}$  one obtains the two equations, describing the evolution of polarization:

$$\begin{aligned} \frac{dP_F(t)}{dt} &= -R_F [P_F(t) - P_{F,eq}] - \\ &\quad -\sigma [P_F(t) - P_H(t)] \\ \frac{dP_H(t)}{dt} &= -R_H [P_H(t) - P_{H,eq}] + \\ &\quad +\sigma \frac{N_F}{N_H} [P_F(t) - P_H(t)] \end{aligned} \quad (6)$$

### ESTIMATE OF SPECTRAL DIFFUSION EFFECT IN AN INHOMOGENEOUS ESR LINE

After excitation by MW irradiation, electron flip-flops cause a hopping state exchange between electron spins. The number of flips it makes before the magnetization has decayed due to longitudinal relaxation  $T_{1e}$  is given by:  $N_h \sim T_{1e}/\tau_c$ , where  $\tau_c$  is the electron correlation time. Therefore the electron frequency after this diffusion process is given by  $\sqrt{\langle \Delta\nu^2 \rangle} \sim D_{ee}\sqrt{N_h} = D_{ee}\sqrt{\frac{T_{1e}}{\tau_c}} \sim 100$  MHz, where the correlation time is estimated as  $\tau_c \sim 1/D_{ee}$ , and  $D_{ee} \sim 3$  MHz is a typical dipolar interaction for [BDPA]=40 mM, and  $T_{1e} \sim 1$  ms [3]. Therefore, under these conditions the width of the hole burnt by the MW irradiation is greater than the width of the BDPA ESR line, resulting in a very efficient saturation of it. For larger values of  $T_{1e} \approx 0.3$  s as extrapolated from ref.[4] data, the width of the hole burnt by the MW irradiation is even larger  $\sqrt{\langle \Delta\nu^2 \rangle} \sim 1000$  MHz.

### ADDITIONAL EVIDENCE FOR A CROSS-RELAXATION BETWEEN $^1\text{H}$ AND $^{19}\text{F}$ NUCLEI

As pointed out in the main text, the cross-relaxation can also be detected in the experiments, where the recovery of  $^1\text{H}$ - and  $^{19}\text{F}$  magnetization is followed after a saturation of  $^{19}\text{F}$ -nuclei by a train of RF pulses. The pulse sequence, and main results are shown in Fig.S2. In addition, cross-relaxation between  $^1\text{H}$  and  $^{19}\text{F}$  can be detected by recording the DNP spectra with a fine step in MW frequency, as shown in Fig.S3.

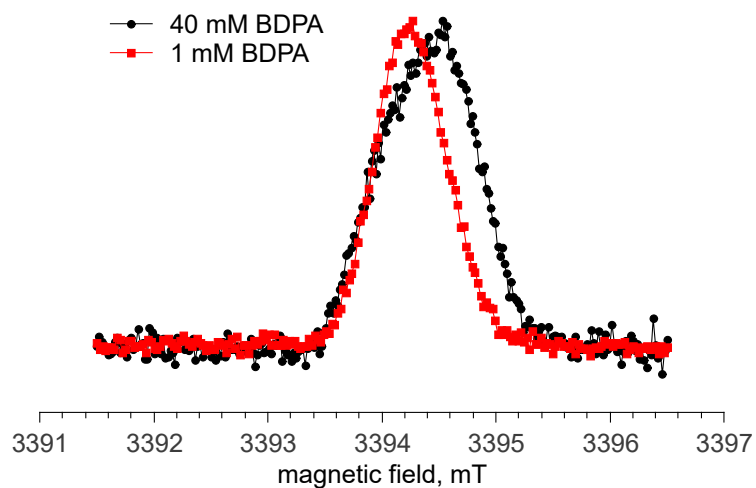


FIG. S1. Field-sweep ESR spectra of BDPA in 25/75 (% v/v) fluorobenzene/toluene recorded for samples of two concentrations. (RED) [BDPA]=1 mM, the detection is performed by integrating the free induction decay signal after a 500 ns  $\pi/2$  pulse. (BLACK) [BDPA]=40 mM, the detection is performed by integrating the echo intensity after  $\pi/2$ - $\tau$ - $\pi/2$ - $\tau$ - $\pi$ - $\tau$ -echo sequence, with  $t_{\pi/2} = 100$  ns,  $t_{\pi} = 200$  ns. Signals are normalized to their respective maximum value.

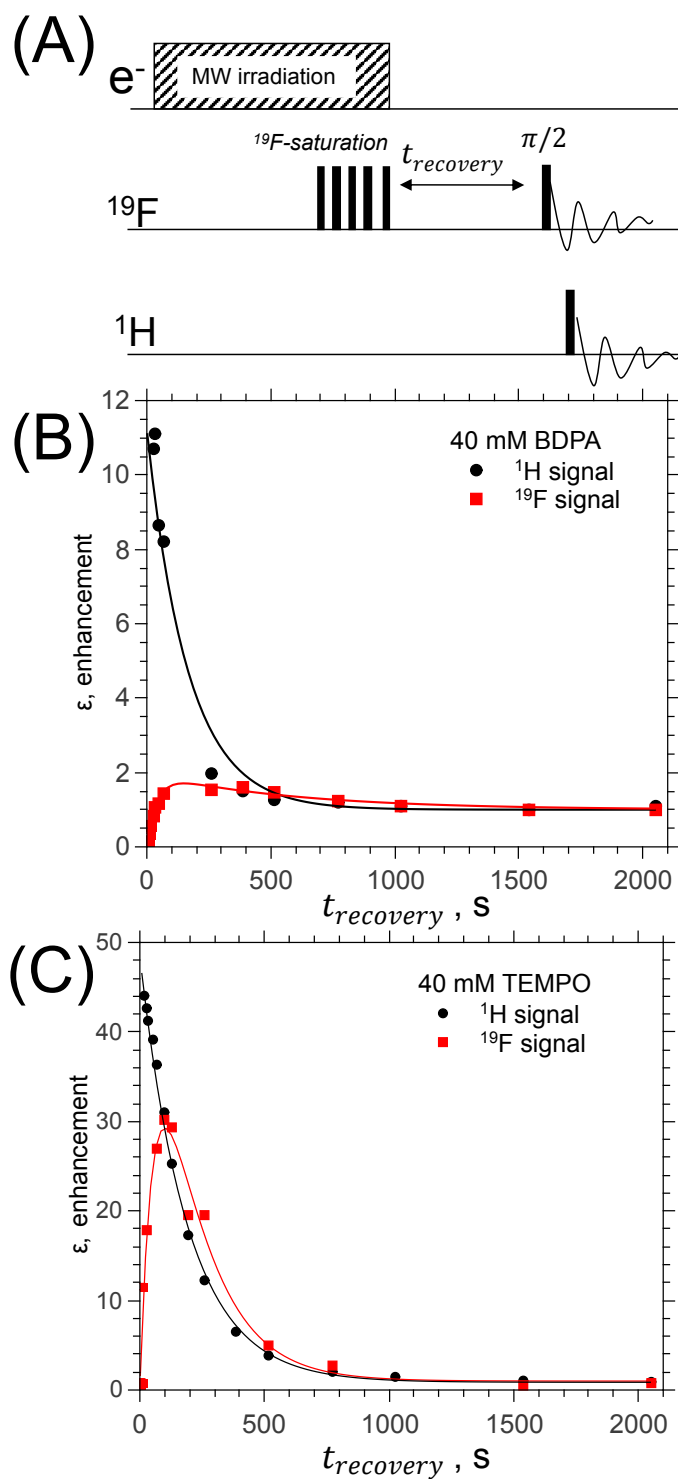


FIG. S2. (A) The pulse sequence for recording the recovery of  $^1\text{H}$ - (red) and  $^{19}\text{F}$ -nuclei to thermal equilibrium after polarizing the nuclei with MW irradiation and saturation of  $^{19}\text{F}$ -nuclei. Recovery of  $^1\text{H}$ - (BLACK) and  $^{19}\text{F}$ -signals (RED) in a sample of 25/75 (% v/v) fluorobenzene/toluene containing (B) [BDPA]=40 mM and (C) [TEMPO]=40 mM (2,2,6,6-tetramethylpiperidine 1-oxyl).

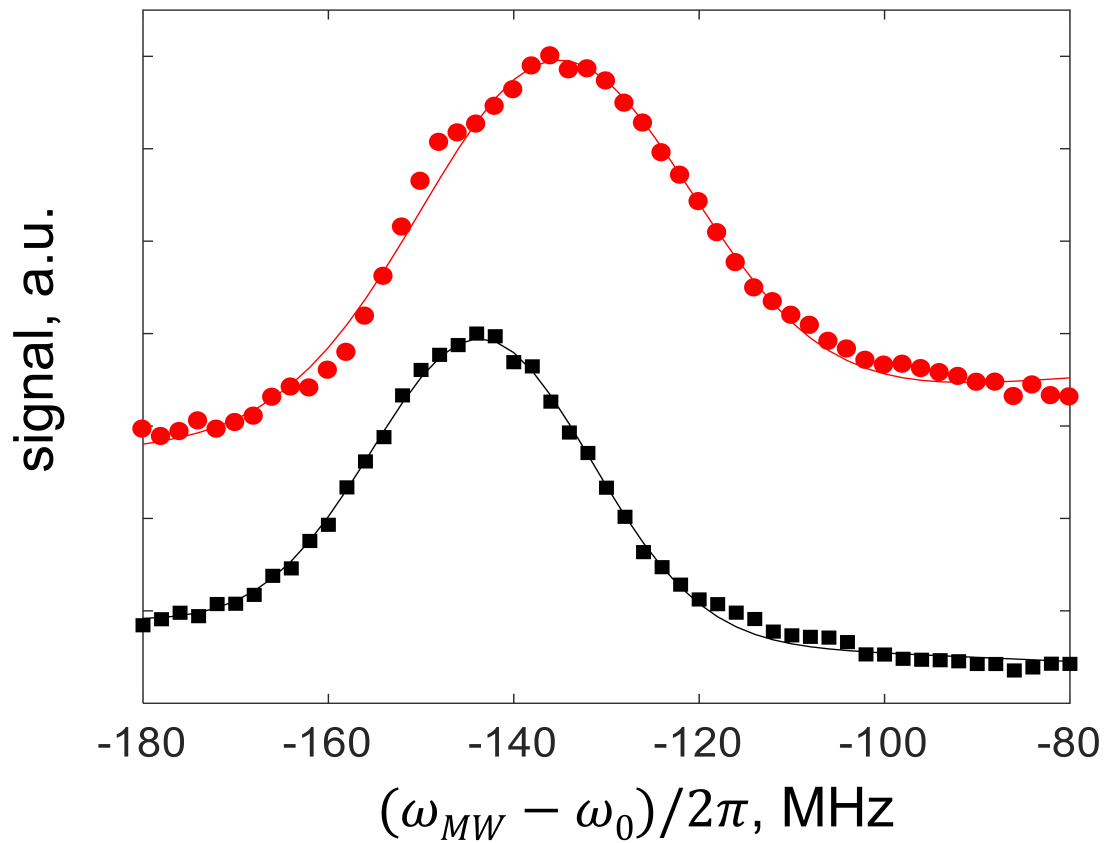


FIG. S3. The DNP spectra of  $^1\text{H}$ - (BLACK) and  $^{19}\text{F}$ -nuclei (RED) recorded after  $t_{bu}=30$  s of build-up for a sample of 25/75 (% v/v) fluorobenzene/toluene containing  $[\text{BDPA}]=40$  mM. The signal intensity is normalized to its maximum value, the horizontal axis is offset by  $\omega_0/2\pi = 93.93$  GHz, the data is recorded in steps of 2 MHz of the microwave frequency  $\omega_{MW}/2\pi$ . Solid lines show the fits with Gaussian functions as explained in the main text.

**MINIMAL MODELS OF SOLID EFFECT,  
HETERONUCLEAR THERMAL MIXING AND  
HETERONUCLEAR CROSS EFFECT DNP**

**Frame Transformation**

In the following section we explain how to obtain an average Hamiltonian  $\hat{H}_{\text{av}}$  that describes both the spin dynamics due to solid effect (SE DNP) and to heteronuclear thermal mixing (hn-TM DNP). In both cases the spin dynamics is described by a zero-quantum Hamiltonian. By transferring the master equation into a frame rotating with the frequencies of these zero-quantum spin transitions oscillating terms in the density operator are generated. We will average the master equation to derive an effective Hamiltonian that describes polarisation transfer due to SE DNP and hn-TM DNP. The zero-quantum transitions are represented by the Hamiltonian  $\hat{H}_0$  which we previously introduced (see Eq. (4) of the main text). The transformed density operator is

$$\hat{\rho} = e^{-i\hat{H}_0 t} \hat{\rho}' e^{i\hat{H}_0 t}.$$

The nuclear polarization dynamics remains unchanged in the new frame, since the operator  $\hat{H}_0$  commutes with the nuclear Zeeman orders  $\hat{I}_{jz}^{(k)}$ ,  $\hat{J}_{jz}^{(l)}$ . The Liouville-von Neumann equation is transformed as

$$d\hat{\rho}/dt = -i[\hat{H}, \hat{\rho}] \quad \longrightarrow \quad d\hat{\rho}'/dt = -i[\hat{H}'(t), \hat{\rho}']$$

where the transformed Hamiltonian  $\hat{H}'(t)$  consists of the time dependent microwave irradiation  $\hat{H}'_{\text{mw}}(t)$  and electron-nuclear interaction  $\hat{H}'_{\text{en}}(t)$  terms

$$\begin{aligned} \hat{H}'(t) &= e^{i\hat{H}_0 t} (\hat{H} - \hat{H}_0) e^{-i\hat{H}_0 t} = \\ &= \hat{H}'_{\text{mw}}(t) + \hat{H}'_{\text{en}}(t) \end{aligned} \quad (7)$$

with

$$\begin{aligned} \hat{H}'_{\text{mw}}(t) &= e^{i\hat{H}_0 t} \hat{H}_{\text{mw}} e^{-i\hat{H}_0 t}, \\ \hat{H}'_{\text{en}}(t) &= e^{i\hat{H}_0 t} \hat{H}_{\text{en}} e^{-i\hat{H}_0 t}. \end{aligned}$$

Using the facts that  $\hat{H}_0$  (see Eq. (5) main text) commutes with  $\hat{H}^0$ , the nuclear Zeeman operators commute with  $\hat{H}_{\text{mw}}$  and the electron Zeeman operators commute with  $\hat{H}_{\text{en}}$  and applying the standard algebraic properties of the spin operators, we obtain

$$\begin{aligned} \hat{H}'_{\text{mw}}(t) &= \frac{\omega_1}{2} \left[ e^{i\Delta t} \sum_j e^{i\hat{H}^0 t} \hat{S}_{j+} e^{-i\hat{H}^0 t} + h.c. \right], \\ \hat{H}'_{\text{en}}(t) &= \frac{1}{2} \left[ e^{i\omega_H t} \sum_{k,j} B_{kj}^{(H)} e^{i\hat{H}^0 t} \hat{I}_{j+}^{(k)} \hat{S}_{jz} e^{-i\hat{H}^0 t} + \right. \\ &\quad \left. + e^{i\omega_F t} \sum_{l,j} B_{lj}^{(F)} J_{j+}^{(l)} e^{i\hat{H}^0 t} \hat{S}_{jz} e^{-i\hat{H}^0 t} + h.c. \right]. \end{aligned} \quad (8)$$

In the next step we consider the microwave irradiation term, that we divide into the secular and non-secular parts

$$\hat{H}'_{\text{mw}}(t) = \hat{H}_{\text{mw}}^0 + \hat{\hat{H}}_{\text{mw}}(t).$$

The secular part

$$\hat{H}_{\text{mw}}^0 = \overline{\hat{H}'_{\text{mw}}(t)} \quad (9)$$

characterizes the constant time average of the operator  $\hat{H}'_{\text{mw}}(t)$  (throughout we use an overline to denote time averages) and the non-secular part  $\hat{\hat{H}}_{\text{mw}}(t)$  describes the oscillating part with zero time average. To take into account the effect that the non-secular part has on the spin dynamics, we apply a methodology similar to the average Hamiltonian theory[5]. More specifically, the Hamiltonian is transformed into the interaction representation frame with respect to  $\hat{\hat{H}}_{\text{mw}}(t)$ , followed by replacing the corresponding transformation operator with the first terms of Magnus expansion. First, we carry out a frame transformation

$$\hat{\rho}' = \hat{U}(t) \hat{\rho}'' \hat{U}^\dagger(t),$$

where the unitary operator  $\hat{U}(t)$  satisfies the equation

$$\dot{\hat{U}} = -i\hat{\hat{H}}_{\text{mw}}(t)\hat{U}, \quad \hat{U}(0) = 1. \quad (10)$$

The Liouville-von Neumann equation is transformed to

$$d\hat{\rho}''/dt = -i[\hat{H}''(t), \hat{\rho}''] \quad \longrightarrow \quad d\hat{\rho}''/dt = -i[\hat{H}''(t), \hat{\rho}'']$$

where the transformed Hamiltonian  $\hat{H}''(t)$  takes the form

$$\begin{aligned} \hat{H}''(t) &= \hat{U}^\dagger(t) \left[ \hat{H}'(t) - \hat{\hat{H}}_{\text{mw}}(t) \right] \hat{U}(t) = \\ &= \hat{U}^\dagger(t) \hat{H}_{\text{mw}}^0 \hat{U}(t) + \hat{U}^\dagger(t) \hat{H}'_{\text{en}}(t) \hat{U}(t). \end{aligned} \quad (11)$$

Since  $\hat{\hat{H}}_{\text{mw}}$  commutes with the nuclear Zeeman orders, the nuclear polarization dynamics in the new frame remains unchanged.

We analyze now under which conditions zero-quantum transitions can be induced by the applied microwave field. According to Eq. (5) in the main text, the operator  $\hat{H}^0$  that we used for the first frame transformation describes the broadening of the electron resonance due to the electron  $g$ -anisotropy, electron dipolar coupling and electron-nuclear hyperfine coupling. The difference between the largest and the smallest eigenvalue of  $\hat{H}^0$ ,  $\Lambda = \lambda_{\text{max}}^0 - \lambda_{\text{min}}^0$  determines the spectral half-width of the electron resonance. At the experimental static magnetic field of  $B_0 = 3.4$  T, the half-width is estimated to be  $\Lambda \sim 20$  MHz, a value much smaller than the nuclear Larmor frequencies  $\omega_H \sim 145$  MHz for  $^1\text{H}$  and  $\omega_F \sim 136$  MHz for  $^{19}\text{F}$  at this field strength. We can then conclude from inspecting Eq. (8) that the non-secular part

$\hat{H}_{\text{mw}}(t)$  of the microwave irradiation term can only be on resonance with the oscillating electron-nuclear term  $\hat{H}'_{\text{en}}(t)$  and induce zero quantum transitions if the microwave frequency offset  $\Delta$  is much larger than  $\lambda_{\text{max}}^0$ , that is well outside the ESR line, and comparable to one of the nuclear frequencies. In this particular case the Hamiltonian represents polarization transfer from the electrons to one of the nuclei by the homonuclear SE. For  $|\Delta| \gg \Lambda$ , the solution to Eq. (10) is well approximated by first terms of Magnus expansion:

$$\hat{U}(t) \sim 1 - i \int_0^t \hat{H}_{\text{mw}}(t') dt'$$

where the deviation of  $\hat{U}(t)$  from the identity operator given by the integral term is small, not exceeding a magnitude  $\sim \omega_1/\Lambda \ll 1$ . Substituting this approximation for  $\hat{U}$  into Eq. (11) enables us to write for  $\hat{H}''$

$$\begin{aligned} \hat{H}''(t) &\sim \hat{H}_{\text{mw}}^0 + \hat{H}'_{\text{en}}(t) + \\ &+ i \left[ \int_0^t \hat{H}_{\text{mw}}(t') dt', \hat{H}_{\text{mw}}^0 + \hat{H}'_{\text{en}}(t) \right] \sim \\ &\sim \hat{H}_{\text{mw}}^0 + \hat{H}'_{\text{en}}(t) + \hat{H}^{\text{SE}} \end{aligned} \quad (12)$$

with

$$\hat{H}^{\text{SE}} = i \overline{\left[ \int_0^t \hat{H}_{\text{mw}}(t') dt', \hat{H}'_{\text{en}}(t) \right]}. \quad (13)$$

Here we neglected the small contribution of  $\hat{H}_{\text{mw}}^0$  in the commutator in Eq. (12) and kept the secular time average part of  $\hat{H}'_{\text{en}}(t)$  in the commutator. The latter represents the effective energy of the electron-nuclear exchange due to SE. The commutator defining  $\hat{H}^{\text{SE}}$  in Eq. (13) can be further modified. According to Eq. (8) and the fact that

$$\omega_{H,F} \gg \Lambda, |B_{k,lj}^{(H,F)}| \quad (14)$$

the electron-nuclear interaction term  $\hat{H}'_{\text{en}}(t)$  is fast oscillating with zero time average. This implies that its time integral is also oscillating without any time evolution. Since the time derivative of an oscillating function has zero time average, we can write

$$\begin{aligned} 0 &= \frac{d}{dt} \left[ \int_0^t \hat{H}_{\text{mw}}(t') dt', \int_0^t \hat{H}'_{\text{en}}(t') dt' \right] = \\ &= \left[ \hat{H}_{\text{mw}}(t), \int_0^t \hat{H}'_{\text{en}}(t') dt' \right] + \\ &+ \left[ \int_0^t \hat{H}_{\text{mw}}(t') dt', \hat{H}'_{\text{en}}(t) \right]. \end{aligned}$$

Hence, Eq. (13) can be rewritten

$$\hat{H}^{\text{SE}} = -i \overline{\left[ \hat{H}_{\text{mw}}(t), \int_0^t \hat{H}'_{\text{en}}(t') dt' \right]}. \quad (15)$$

Eq. (12) contains still the fast oscillating term  $\hat{H}'_{\text{en}}(t)$ . An adiabatic elimination can be carried out using the Krylov-Bogolyubov averaging procedure described in our previous works [7, 8] to obtain an effective time-independent term. This procedure uses the Fourier expansion

$$\hat{H}'_{\text{en}}(t) = \sum_s \left( \hat{G}_s e^{i\lambda_s t} + \hat{G}_s^\dagger e^{-i\lambda_s t} \right) \quad (16)$$

where the eigenvalue set  $\{\lambda_s > 0\}$  represents the positive part of the spectrum of the operator  $\hat{H}'_{\text{en}}(t)$ . The first order Krylov-Bogolyubov approximation is the time average of  $\hat{H}'_{\text{en}}(t)$  that is zero, so the first adiabatic approximation is given by the second order Krylov-Bogolyubov approximation

$$\hat{H}_{\text{hnTM}}^{\text{en}} = \sum_s \lambda_s^{-1} \left[ \hat{G}_s, \hat{G}_s^\dagger \right]. \quad (17)$$

As we will discuss below, this term of the Hamiltonian describes the effective energy of the electron-nuclear exchange due to hn-TM DNP. It is important to point out, that the same result could be obtained by applying a Floquet transformation, followed by Van Vleck's perturbation theory to obtain the effective Hamiltonian[6]. The Eq. (17) is essentially a multifrequency (or multi-mode) analogue of the first term of effective Floquet Hamiltonian.

Combining the microwave, SE and hn-TM contributions (9), (15), (17), this leads to the effective time independent average Hamiltonian that describes the electron-nuclear BDPA -  $^1\text{H}$  -  $^{19}\text{F}$  spin dynamics

$$\hat{H}_{\text{av}} = \hat{H}_{\text{mw}}^0 + \hat{H}_{\text{SE}} + \hat{H}_{\text{hnTM}}^{\text{en}}. \quad (18)$$

The rest of this section is devoted to the estimation of the components of the average Hamiltonian (18) in terms of the system parameters and properties of the ESR line. We will also derive the minimal SE-hn-TM model described in the main text.

### Average Hamiltonian for SE DNP

Introducing the notation for the spin operators after transformation to the frame rotating with the frequency of the zero-quantum coherences

$$\begin{aligned} \hat{S}'_{j+}(t) &\equiv e^{i\hat{H}^0 t} \hat{S}_{j+} e^{-i\hat{H}^0 t}, \\ \hat{I}'_{j\pm}(k) \hat{S}'_{j+}(t) &\equiv e^{i\hat{H}^0 t} \hat{I}'_{j\pm}(k) \hat{S}_{j+} e^{-i\hat{H}^0 t}, \\ \hat{I}'_{j+}(k) \hat{S}'_{jz}(t) &\equiv e^{i\hat{H}^0 t} \hat{I}'_{j+}(k) \hat{S}_{jz} e^{-i\hat{H}^0 t}, \\ \hat{S}'_{jz}(t) &\equiv e^{i\hat{H}^0 t} \hat{S}_{jz} e^{-i\hat{H}^0 t}, \end{aligned} \quad (19)$$



it follows from Eqs. (8), (9) and (19)

$$\hat{H}_{\text{mw}}^0 = \frac{\omega_1}{2} \left[ \sum_j \overline{e^{i\Delta t} \hat{S}'_{j+}(t)} + h.c. \right]. \quad (20)$$

In accordance with Eq. (8), (14), the operator  $\hat{H}_{\text{en}}(t)$  is fast oscillating with (apart from a non-important constant shift)

$$\int_0^t \hat{H}'_{\text{en}}(t') dt' \sim \frac{1}{2} \left[ \frac{e^{i\omega_H t}}{i\omega_H} \sum_{k,j} B_{kj}^{(H)} e^{i\hat{H}^0 t} \hat{I}_{j+}^{(k)} \hat{S}'_{jz} e^{-i\hat{H}^0 t} + \frac{e^{i\omega_F t}}{i\omega_F} \sum_{l,j} B_{lj}^{(F)} \hat{J}_{j+}^{(l)} e^{i\hat{H}^0 t} \hat{S}'_{jz} e^{-i\hat{H}^0 t} + h.c. \right].$$

Eqs. (8) and (15) give then

$$\begin{aligned} \hat{H}_{\text{SE}} = & \frac{\omega_1}{4} \left[ \frac{1}{\omega_H} \sum_{k,j} B_{kj}^{(H)} \overline{e^{i(\Delta+\omega_H)t} \hat{I}_{j+}^{(k)} \hat{S}'_{j+}(t)} + \right. \\ & + \frac{1}{\omega_H} \sum_{k,j} B_{kj}^{(H)*} \overline{e^{i(\Delta-\omega_H)t} \hat{I}_{j-}^{(k)} \hat{S}'_{j+}(t)} + \\ & + \frac{1}{\omega_F} \sum_{l,j} B_{lj}^{(F)} \hat{J}_{j+}^{(l)} \overline{e^{i(\Delta+\omega_F)t} \hat{S}'_{j+}(t)} + \\ & \left. + \frac{1}{\omega_F} \sum_{l,j} B_{lj}^{(F)*} \hat{J}_{j-}^{(l)} \overline{e^{i(\Delta-\omega_F)t} \hat{S}'_{j+}(t)} + h.c. \right]. \end{aligned} \quad (21)$$

It follows also from Eqs. (8) and (19)

$$\begin{aligned} \hat{H}'_{\text{en}}(t) = & \frac{1}{2} \left[ e^{i\omega_H t} \sum_{k,j} B_{kj}^{(H)} \hat{I}_{j+}^{(k)} \hat{S}'_{jz}(t) + \right. \\ & \left. + e^{i\omega_F t} \sum_{l,j} B_{lj}^{(F)} \hat{J}_{j+}^{(l)} \hat{S}'_{jz}(t) + h.c. \right]. \end{aligned} \quad (22)$$

The time-averaged terms in Eq. (21) can be simplified further by analysing the frequency spectrum of the oscillations that arise from the transformation into the zero-quantum frame (Eq. (7)). We will show that rather than keeping track of each frequency it is possible to replace the oscillating terms by spectral densities. We start in the spectral analysis with the operator  $\hat{S}'_{j+}(t)$  that generates the Fourier expansion

$$\hat{S}'_{j+}(t) = \sum_s f_{js} \hat{O}_{js} e^{i\lambda_s t}$$

where the set of real frequencies  $\{\lambda_s\}$  is given by differences  $\lambda_q^0 - \lambda_{q'}^0$  of the eigenvalues of the operator  $\hat{H}^0$ . The amplitudes  $f_{js} \hat{O}_{js}$  are generated by the off-diagonal matrix elements of the operator  $\hat{S}'_{j+}$  in the basis of eigenstates of  $\hat{H}^0$ . Here  $f_{js}$  is the factor that depends on the frequency  $\lambda_s$ . It is possible to replace this discrete Fourier

expansion by its integral approximation if the spectrum of operator  $\hat{S}'_{j+}(t)$  is sufficiently dense. Introducing the average frequency difference  $\nu$  between two consecutive eigenvalues of the set  $\{\lambda_s\}$ , we can approximate the frequencies as  $\lambda_s = s\nu$  where the integer  $s$  runs through the interval  $[-s_+, s_+]$  with  $s_+\nu = \Lambda \equiv \max |\lambda_s|$  determined by the half-width of the spectrum  $\Lambda$ . In other words, if the spectrum of the operator  $\hat{S}'_{j+}(t)$  is sufficiently dense, we can replace the set  $\{\lambda_s\}$  by a new set of equally spaced frequencies. If  $\nu \ll \Lambda$  and  $s_+ \gg 1$  we can write

$$\hat{S}'_{j+}(t) = \sum_{s=-s_+}^{s_+} f_j(s\nu) \hat{O}_{js} e^{is\nu t} \sim \frac{1}{\nu} \int_{-\infty}^{+\infty} f_j(\lambda) \hat{O}'_j e^{i\lambda t} d\lambda. \quad (23)$$

Here  $f_j(\lambda)$  is the dimensionless continuous envelope spectral density function that approximates the amplitudes  $f_{js} = f_j(s\nu)$  and  $\hat{O}'_j$  is a frequency independent operator that satisfies Eq. (23). We can find  $\hat{O}'_j$  by setting  $t = 0$ :

$$\hat{S}'_{j+}(0) = \hat{S}_{j+} \sim \left( \frac{1}{\nu} \int_{-\infty}^{+\infty} f_j(\lambda) d\lambda \right) \hat{O}'_j$$

from which we can conclude that  $\hat{O}'_j = \hat{S}_{j+}$  if  $\frac{1}{\nu} \int_{-\infty}^{+\infty} f_j(\lambda) d\lambda \sim 1$ , which is equivalent to requiring that the zeroth moment of the spectral density function  $\mu_0[f_j(\lambda)] = 1$ . We can then approximate  $\hat{S}'_{j+}(t)$  by

$$\hat{S}'_{j+}(t) = \left( \frac{1}{\nu} \int_{-\infty}^{+\infty} f_j(\lambda) e^{i\lambda t} d\lambda \right) \hat{S}_{j+}. \quad (24)$$

Following an identical set of arguments we find for  $\hat{I}_{j\pm}^{(k)} \hat{S}'_{j+}(t)$  that

$$\hat{I}_{j\pm}^{(k)} \hat{S}'_{j+}(t) = \left( \frac{1}{\nu} \int_{-\infty}^{+\infty} f'_{kj}(\lambda) e^{i\lambda t} d\lambda \right) \hat{I}_{j\pm}^{(k)} \hat{S}_{j+}, \quad (25)$$

where  $f'_{kj}(\lambda)$  is another spectral density function with zeroth moment  $\mu_0[f'_{jk}(\lambda)] = 0$

Using then the following shift formula that is valid for any frequency  $\omega$  and any spectral density function  $f(\lambda)$ ,

$$\overline{e^{i\omega t} \int_{-\infty}^{+\infty} f(\lambda) e^{i\lambda t} d\lambda} = \int_{-\infty}^{+\infty} f(\lambda - \omega) e^{i\lambda t} d\lambda = f(-\omega).$$

and substituting (31) and (25) into Eqs. (20), (21), we obtain the following estimates for the microwave and SE parts of the average Hamiltonian

$$\hat{H}_{\text{mw}}^0 = \frac{\omega_1}{2} \left[ \sum_j f_j(\Delta) \hat{S}_{j+} + h.c. \right], \quad (26)$$

$$\begin{aligned}
\hat{H}_{SE} = & \frac{\omega_1}{4} \left[ \frac{1}{\omega_H} \sum_{k,j} B_{kj}^{(H)} f'_{kj}(\Delta + \omega_H) I_{j+}^{(k)} \hat{S}_{j+} + \right. \\
& + \frac{1}{\omega_H} \sum_{k,j} B_{kj}^{(H)*} f'_{kj}(\Delta - \omega_H) \hat{I}_{j-}^{(k)} \hat{S}_{j+} + \\
& + \frac{1}{\omega_F} \sum_{l,j} B_{lj}^{(F)} f_j(\Delta + \omega_F) \hat{J}_{j+}^{(l)} \hat{S}_{j+} + \\
& \left. + \frac{1}{\omega_F} \sum_{l,j} B_{lj}^{(F)*} f_j(\Delta - \omega_F) \hat{J}_{j-}^{(l)} \hat{S}_{j+} + h.c. \right]
\end{aligned} \tag{27}$$

where we inverted the argument  $\lambda \rightarrow -\lambda$  of the spectral densities  $f_j(\lambda)$ ,  $f'_{kj}(\lambda)$ .

### Properties of the Spectral Densities $f_j(\lambda)$ and $f'_{kj}(\lambda)$

To characterise the shape of the spectral density function  $f_j(\lambda)$  we can calculate its moments

$$\mu_r[f_j] = \frac{1}{\nu} \int_{-\infty}^{+\infty} \lambda^r f_j(\lambda) d\lambda, \quad r = 0, 1, \dots,$$

using the time derivatives of the operator  $\hat{S}'_{j+}(0) = \hat{S}_{j+}$ . It follows from Eq. (19) and Eq. (23) that the first time derivative at  $t = 0$  gives

$$\begin{aligned}
\frac{d}{dt} \hat{S}'_{j+}(0) &= i [\hat{H}^0, \hat{S}_{j+}] = \\
&= \left[ \Delta_j^{(g)} + \sum_k A_{kj} \hat{I}_{jz}^{(k)} + 2 \sum_{j' \neq j} D_{jj'} \hat{S}_{j'z} \right] \hat{S}_{j+} + \\
&\quad + \sum_{j' \neq j} D_{jj'} \hat{S}_{jz} \hat{S}_{j'+}.
\end{aligned} \tag{28}$$

The second time derivative at  $t = 0$  provides

$$\begin{aligned}
\frac{d^2}{dt^2} \hat{S}_{j+}(0) &= -[\hat{H}^0, [\hat{H}^0, \hat{S}_{j+}]] = \\
&= \left[ \left( \Delta_j^{(g)} \right)^2 + \frac{1}{4} \sum_k A_{kj}^2 \right] \hat{S}_{j+} + \\
&\quad + \sum_{j' \neq j} D_{jj'}^2 \left( \frac{5\hat{S}_{j+}}{4} + \hat{S}_{j'+} \right).
\end{aligned} \tag{29}$$

For simplicity, in the last formula we kept only single-spin orders. The moments  $\mu_r(f_j)$  are then obtained from Eq. (28) and Eq. (29) by factoring out  $\hat{S}_{j+}$  and using the remaining terms

$$\begin{aligned}
\mu_1[f_j] &= \frac{1}{\nu} \int_{-\infty}^{+\infty} \lambda f_j(\lambda) d\lambda \sim \\
&\sim \Delta_j^{(g)} + \sum_k A_{kj} \hat{I}_{jz}^{(k)} + 3 \sum_{j' \neq j} D_{jj'} \hat{S}_{j'z}, \\
\mu_2[f_j] &= \frac{1}{\nu} \int_{-\infty}^{+\infty} \lambda^2 f_j(\lambda) d\lambda \sim \\
&\sim \left( \Delta_j^{(g)} \right)^2 + \frac{1}{4} \sum_k A_{kj}^2 + \frac{9}{4} \sum_{j' \neq j} D_{jj'}^2.
\end{aligned} \tag{30}$$

The first moment  $\mu_1[f_j]$  determines the mean of the spectral density  $f_j(\lambda)$ , i.e. the position of its peak. The magnitude  $(\mu_2[f_j] - \mu_1^2[f_j])^{1/2}$  determines its dispersion, i.e., the half-width of  $f_j(\lambda)$ . For BDPA radicals [9], the electron hyperfine coupling to the structural  $^1\text{H}$  spins, defined by the set of coefficients  $A_{kj}$ , dominates over the electron-electron coupling with the coefficients  $D_{jj'}$  and the  $g$ -anisotropy shift  $\Delta_j^{(g)}$ . According to Eq. (30), the spectral density  $f_j(\lambda)$  is composed by a set of lines with peaks determined by the hyperfine distribution  $A_{kj} \hat{I}_{jz}^{(k)}$  and broadened by the electron-electron coupling. The set  $\{A_{kj} \hat{I}_{jz}^{(k)}\}$  arises from 8 nuclear  $^1\text{H}$  spins of the biphenyl rings with dominating coupling to the unpaired electron [9]. Because of the anisotropy of the hyperfine coupling, all possible orientations of the dominating 8 structural  $^1\text{H}$  spins generate a highly dense set of lines that is symmetric with respect to zero ( $\lambda = 0$ ). The characteristic frequency difference between two consecutive eigenvalues of the spectrum,  $\nu \sim \Lambda/2^8 \sim 20/256 \text{ MHz} \sim 0.1 \text{ MHz}$  is smaller than the average coupling strength between the neighbouring electrons for an experimental 40 mM radical concentration,  $D_0 \sim 0.3 \text{ MHz}$ . Hence, the lines generated by the hyperfine coupling distribution  $\{A_{kj}\}$  well overlap, forming an effective continuous envelope. This mean  $\mu_1[f_j]$  of spectral density  $f_j(\lambda)$  can be estimated using Eq. (30) neglecting the contribution of the hyperfine interaction due to the fact that  $\hat{I}_{jz}^{(k)} = \pm 1/2$ . The variance, however, keeps the corresponding hyperfine term. We can write with a good accuracy

$$\begin{aligned}
\mu_1[f_j] &= \frac{1}{\nu} \int_{-\infty}^{+\infty} \lambda f_j(\lambda) d\lambda \sim \\
&\sim \Delta_j^{(g)} + 3 \sum_{j' \neq j} D_{jj'} \hat{S}_{j'z}, \\
\sigma^2[f_j] &= -\mu_1^2[f_j] + \frac{1}{\nu} \int_{-\infty}^{+\infty} \lambda^2 f_j(\lambda) d\lambda \sim \\
&\sim \frac{1}{4} \sum_k A_{kj}^2 + \frac{9}{4} \sum_{j' \neq j} D_{jj'}^2.
\end{aligned} \tag{31}$$

Similarly, we obtain for  $f'_{kj}$  in Eq. (25)

$$\begin{aligned}
\mu_1[f'_{kj}] &= \frac{1}{\nu} \int_{-\infty}^{+\infty} \lambda f'_{kj}(\lambda) d\lambda \sim \\
&\sim \Delta_j^{(g)} + 3 \sum_{j' \neq j} D_{jj'} \hat{S}_{j'z}, \\
\sigma^2[f'_{kj}] &= -\mu_1^2[f'_{kj}] + \frac{1}{\nu} \int_{-\infty}^{+\infty} \lambda^2 f'_{kj}(\lambda) d\lambda \sim \\
&\sim \frac{1}{4} \sum_{k' \neq k} A_{kj}^2 + \frac{9}{4} \sum_{j' \neq j} D_{jj'}^2.
\end{aligned} \tag{32}$$

where we took into account the fact that the hyperfine coupling  $A_{kj} \hat{I}_{jz}^{(k)} \hat{S}_{jz}$  of the  $k$ th  $^1\text{H}$  nucleus commutes with the operators  $\hat{I}_{j\pm}^{(k)} \hat{S}_{j+}$  leading to a slightly narrower density  $f'_{kj}(\lambda)$  compared with  $f_j(\lambda)$ .

### Average Hamiltonian for hn-TM DNP

We proceed now to the evaluation of the hn-TM part of the average Hamiltonian (18) using Eqs. (16) and (17). According to Eq. (19), the time derivative of the sandwich  $\hat{S}'_{jz}(t)$  takes the form

$$\begin{aligned} \frac{d}{dt}\hat{S}'_{jz}(t) &= ie^{i\hat{H}^0 t} \left[ \hat{H}^0, \hat{S}_{jz} \right] e^{-i\hat{H}^0 t} = \\ &= \frac{i}{2} \sum_{j' \neq j} D_{jj'} e^{iH^0 t} \left( \hat{S}_{j+} \hat{S}'_{j'-} - h.c. \right) e^{-i\hat{H}^0 t} = \\ &= \frac{i}{2} \sum_{j' \neq j} D_{jj'} \left[ \hat{S}'_{j+}(t) \hat{S}'_{j'-}(t) - h.c. \right]. \end{aligned} \quad (33)$$

Using the result in Eq. (31) we get

$$\hat{S}'_{j+}(t) \hat{S}'_{j'-}(t) = \left( \frac{1}{\nu} \int_{-\infty}^{+\infty} F_{jj'}(\lambda) e^{i\lambda t} d\lambda \right) \hat{S}_{j+} \hat{S}_{j'-} \quad (34)$$

where the spectral density  $F_{jj'}(\lambda)$  is given by the convolution of the two spectral densities  $f_j(\lambda)$ ,  $f_{j'}(\lambda)$  previously introduced,

$$F_{jj'}(\lambda) = \frac{1}{\nu} \int_{-\infty}^{+\infty} f_j(\lambda') f_{j'}^\dagger(\lambda' - \lambda) d\lambda'. \quad (35)$$

Similarly, utilizing Eqs. (19), (25) and neglecting a small frequency shift caused by the hyperfine coupling  $A_{kj}$ ,

$$\begin{aligned} \frac{d}{dt} \hat{I}_{j+}^{(k)} \hat{S}'_{jz}(t) &= ie^{i\hat{H}^0 t} \left[ \hat{H}^0, \hat{I}_{j+}^{(k)} \hat{S}_{jz} \right] e^{-i\hat{H}^0 t} = \\ &+ \frac{i}{2} \sum_{j' \neq j} D_{jj'} e^{i\hat{H}^0 t} \hat{I}_{j+}^{(k)} \left( \hat{S}_{j+} \hat{S}'_{j'-} - h.c. \right) e^{-i\hat{H}^0 t} = \\ &= \frac{i}{2} \sum_{j' \neq j} D_{jj'} \left[ \hat{I}_{j+}^{(k)} \hat{S}'_{j+}(t) \hat{S}'_{j'-}(t) - \hat{I}_{j-}^{(k)} \hat{S}'_{j+}(t) \hat{S}'_{j'+}(t) \right]. \end{aligned} \quad (36)$$

where

$$\begin{aligned} \hat{I}_{j+}^{(k)} \hat{S}'_{j+}(t) \hat{S}'_{j'-}(t) &= U_{kjj'}(t) \hat{I}_{j+}^{(k)} \hat{S}_{j+} \hat{S}_{j'-}, \\ \hat{I}_{j-}^{(k)} \hat{S}'_{j+}(t) \hat{S}'_{j'+}(t) &= U_{kjj'}^\dagger(t) \hat{I}_{j+}^{(k)} \hat{S}_{j-} \hat{S}_{j'+}, \\ U_{kjj'}(t) &= \frac{1}{\nu} \int_{-\infty}^{+\infty} F'_{kjj'}(\lambda) e^{i\lambda t} d\lambda, \\ F'_{kjj'}(\lambda) &= \frac{1}{\nu} \int_{-\infty}^{+\infty} f'_{kj}(\lambda') f_{j'}^\dagger(\lambda' - \lambda) d\lambda'. \end{aligned} \quad (37)$$

The time integration of Eqs. (33) and (36) returns the estimates

$$\begin{aligned} \hat{S}'_{jz}(t) &= \hat{S}_{jz} + \frac{i}{2} \sum_{j' \neq j} D_{jj'} \left[ \int_0^t \hat{S}'_{j+}(t') \hat{S}'_{j'-}(t') dt' - h.c. \right], \\ \hat{I}_{j+}^{(k)} \hat{S}'_{jz}(t) &= \hat{I}_{j+}^{(k)} \hat{S}_{jz} + \\ &+ \frac{i}{2} \sum_{j' \neq j} D_{jj'} \left[ \int_0^t \hat{I}_{j+}^{(k)} \hat{S}'_{j+}(t') \hat{S}'_{j'-}(t') dt' - h.c. \right]. \end{aligned}$$

The two oscillating terms in Eq. (22) can be replaced using spectral densities

$$\begin{aligned} e^{i\omega_F t} \hat{S}'_{jz}(t) &\longrightarrow \delta(\lambda - \omega_F) \hat{S}_{jz} + \\ &+ \frac{1}{2} \sum_{j' \neq j} D_{jj'} \left[ \frac{F_{jj'}(\lambda - \omega_F)}{\lambda - \omega_F} \hat{S}_{j+} \hat{S}'_{j'-} + \right. \\ &\quad \left. + \frac{F_{jj'}^\dagger(\omega_F - \lambda)}{\omega_F - \lambda} \hat{S}_{j-} \hat{S}'_{j'+} \right] \\ e^{i\omega_H t} \hat{I}_{j+}^{(k)} \hat{S}'_{jz}(t) &\longrightarrow \delta(\lambda - \omega_H) \hat{I}_{j+}^{(k)} \hat{S}_{jz} + \\ &+ \frac{1}{2} \sum_{j' \neq j} D_{jj'} \hat{I}_{j+}^{(k)} \left[ \frac{F'_{kjj'}(\lambda - \omega_H)}{\lambda - \omega_H} \hat{S}_{j+} \hat{S}'_{j'-} + \right. \\ &\quad \left. + \frac{F'_{kjj'}^\dagger(\omega_H - \lambda)}{\omega_H - \lambda} \hat{S}_{j-} \hat{S}'_{j'+} \right], \end{aligned} \quad (38)$$

where  $\delta(\lambda)$  is the Dirac delta-function and  $F_{jj'}(\lambda)$ ,  $F'_{kjj'}(\lambda)$  are defined by Eqs. (35), (37). Eqs. (16), (17) and (38) can then be combined to obtain an estimate of the hn-TM part of the average Hamiltonian

$$\begin{aligned} \hat{H}_{\text{hnTM}}^{\text{en}} &= -\frac{1}{8\omega_H\omega_F} \sum_{k,l,j,j'} \hat{W}_{jj'}^{(kl)} \hat{S}_{j+} \hat{S}_{j'-} + h.c., \\ \hat{W}_{jj'}^{(kl)} &= D_{jj'} \left[ g_{jj'}^+ \hat{V}_{jj'}^{(kl)} + g_{jj'}^- \hat{V}_{jj'}^{(kl)\dagger} \right], \\ \hat{V}_{jj'}^{(kl)} &= B_{kj}^{(H)} \hat{I}_{j+}^{(k)} \left[ B_{lj}^{(F)*} \hat{J}_{j-}^{(l)} - B_{lj}^{(F)*} \hat{J}_{j-}^{(l)} \right], \\ g_{jj'}^\pm &= F_{jj'}(\mp\omega), \quad \omega = \omega_H - \omega_F \end{aligned} \quad (39)$$

where the density  $F_{jj'}(\lambda)$  is given by Eq. (35) and for simplicity we neglected the small difference between the widths of the densities  $f_j(\lambda)$ ,  $f'_{kj}(\lambda)$  given by Eqs. (31), (25).

### Symmetry Breaking and Minimal Model

The four-spin flips  $\hat{I}_{j\pm}^{(k)} \hat{J}_{j\mp}^{(l)} \hat{S}_{j+} \hat{S}_{j'-}$  and their Hermitian conjugates, in the hn-TM term given by Eq. (39) mediate the polarization transfer of the difference of electron polarization to the polarization differences of the nuclear species. This gives rise to peaks of opposite signs for  $^1\text{H}$  and  $^{19}\text{F}$  nuclei near the electron microwave offset, comparable to the half-width of the ESR line: positive  $^{19}\text{F}$  and negative  $^1\text{H}$  peaks for  $\Delta \sim \Lambda$  and positive  $^1\text{H}$  and negative  $^{19}\text{F}$  peaks for  $\Delta \sim -\Lambda$ . The prerequisites for the electron-nuclear polarization transfer is the dispersion of the microscopic electron spectral densities  $f_j(\lambda)$  between the electron spins and the fact that the nuclear frequency difference  $\omega$  is appreciably smaller than the ESR line half-width. At a given electron offset  $\Delta$ , different electron spins have different effective microwave field strengths  $\omega_1 f_j(\Delta)$  and the microwave term  $\hat{H}_{\text{mw}}^0$  creates polarization differences between them. The dispersion of  $f_j(\lambda)$  along with the fact that  $\omega < \Lambda$  causes the

asymmetry  $|g_{jj'}^+| \neq |g_{jj'}^-|$ , so the electron nuclear four-spin flips that compose the  $\hat{H}_{\text{hnTM}}$  part of the average Hamiltonian (18) create the net polarization difference between  $^1\text{H}$  and  $^{19}\text{F}$  nuclear species. Due to the relation  $g_{jj'}^+ = g_{j'j}^-$ , the  $(jj')$  and  $(j'j)$  electron pairs generate the same enhancements of the nuclei attached to the  $j$ th and  $j'$ th electrons where the nuclear species with the smaller/larger Larmor frequency gets a positive/negative polarization enhancement for  $\Delta \sim \Lambda$ , opposite to the enhancements for  $\Delta \sim -\Lambda$ .

As seen from Eq. (31), the dispersion of the microscopic electron densities  $f_j(\lambda)$  is a combination of the electron  $g$ -anisotropy and dispersion of the electron-electron dipolar coupling. In fact, even in the absence of the  $\Delta_j^{(g)}$ , the means of the spectral densities  $f_j(\lambda)$ ,  $f_{j'}(\lambda)$  of two electron spins correlate via the presence of the coupling with other electrons. As a result, unlike the hyperfine terms, the electron coupling terms  $\sum D_{jj'} \hat{S}_{j'z}$  are not averaged out by different orientations  $\hat{S}_{j'z} = \pm 1/2$  and participate in creating differences between the means of the densities  $f_j(\lambda)$  that result in the creation of electron polarization differences. We can assume that each  $f_j(\lambda)$  has roughly the same variance, caused mainly by the hyperfine coupling that dominates in the ESR linewidth.

To describe the macroscopic electron-nuclear dynamics due to hn-TM, we use the minimal model Hamiltonian that involves two effective electron spins and two effective unlike nuclear spins, with electron microwave irradiation and electron-nuclear flip-flop terms utilizing the width of the electron resonance and a dispersion arising from the electron dipolar coupling and possible electron  $g$ -anisotropy. Since the electron polarization gradients created by the microwave are transferred to the nuclei in an effective two-electron two-nuclear process, the chosen four-spin model is the minimal model that describes the hn-TM mechanism. As the characteristic spectral densities  $f_j(\Delta)$  of this minimal two-electron model, we use the shapes given by Eq. (31) with the maximal positive and maximal negative means  $\mu_1[f_j]$  and the same variance  $\sigma^2[f_j]$ . The variance is given roughly by the width of the ESR line dominated by the hyperfine coupling and influenced also by the electron-electron dipolar coupling, as described in Eq. (31). According to the same equation, the minimal and maximal means are written as  $\max \mu_1[f_j] = d$ ,  $\min \mu_1[f_j] = -d$  where  $d$  is determined by the combined dispersion of the electron  $g$ -anisotropy and the electron-electron dipolar coupling

$$d = \max_j \left| \Delta_j^{(g)} + \frac{3}{2} \sum_{j' \neq j} D_{jj'} \right|.$$

From Eq. (39) we obtain the effective minimal hn-TM

Hamiltonian

$$\begin{aligned} \hat{H}_{\text{hnTM}} &= \hat{H}_{\text{hnTM}}^{\text{mw}} + \hat{H}_{\text{hnTM}}^{\text{en}}, \\ \hat{H}_{\text{hnTM}}^{\text{mw}} &= \omega_1 \left[ f_+(\Delta) \hat{S}_{1x} + f_-(\Delta) \hat{S}_{2x} \right], \\ \hat{H}_{\text{hnTM}}^{\text{en}} &= -\frac{DB^{(H)}B^{(F)}}{\omega_H\omega_F} \left[ g_+ \hat{I}_+ \hat{J}_- + \right. \\ &\quad \left. + g_- \hat{I}_- \hat{J}_+ \right] \hat{S}_{1+} \hat{S}_{2-} + h.c., \\ f_{\pm}(\Delta) &= f(\Delta \pm d), \\ g_+ &= \frac{1}{\nu} \int_{-\infty}^{+\infty} f_-(\Delta) f_+(\Delta - \omega) d\Delta, \\ g_- &= \frac{1}{\nu} \int_{-\infty}^{+\infty} f_+(\Delta) f_-(\Delta - \omega) d\Delta, \\ \omega &= \omega_H - \omega_F. \end{aligned} \quad (40)$$

Here  $\omega_1$  is the microwave field strength,  $\omega_{H,F}$  are the nuclear frequencies,  $D$ ,  $B^{(H,F)}$  are the effective electron-electron and electron-nuclear interaction strengths respectively,  $f$  is a density normalized ESR lineshape of a width  $A$  and  $d$  is the dispersion magnitude.

Due to the presence of two-spin flips  $\hat{I}_{j\pm}^{(k)} \hat{S}_{j\pm}$ ,  $\hat{J}_{j\pm}^{(l)} \hat{S}_{j\pm}$  and their Hermitian conjugates, the SE term given by Eq. (27) causes the polarization transfer from single electron spins to  $^1\text{H}$  and  $^{19}\text{F}$  nuclear spin species, with negative peaks of the same sign for  $\Delta \sim \omega_{H,F}$  and positive peaks of the same sign for  $\Delta \sim -\omega_{H,F}$ . To describe the macroscopic electron-nuclear dynamics due to SE, we use the minimal model Hamiltonian that involves a single electron spin and two effective unlike nuclear spins, with electron microwave irradiation and electron-nuclear terms utilizing the width of the electron resonance,

$$\begin{aligned} \hat{H}_{\text{SE}} &= \hat{H}_{\text{SE}}^{\text{mw}} + \hat{H}_{\text{SE}}^{\text{en}}, \\ \hat{H}_{\text{SE}}^{\text{mw}} &= \omega_1 f(\Delta) \hat{S}_x, \\ \hat{H}_{\text{SE}}^{\text{en}} &= -\frac{\omega_1}{4\Delta} \left[ B^{(H)} \left( f_H^+(\Delta) \hat{I}_+ \hat{S}_+ + f_H^-(\Delta) \hat{I}_- \hat{S}_+ \right) \right. \\ &\quad \left. + B^{(F)} \left( f_F^+(\Delta) \hat{J}_+ \hat{S}_+ + f_F^-(\Delta) \hat{J}_- \hat{S}_+ \right) \right] + h.c., \\ f_H^{\pm}(\Delta) &= f(\Delta \pm \omega_H), \\ f_F^{\pm}(\Delta) &= f(\Delta \pm \omega_F). \end{aligned} \quad (41)$$

For simplicity, we use in Eq. (41) the same electron-nuclear interaction strengths  $B^{(H)}, B^{(F)}$  as in the hn-TM model (40).

### The Heteronuclear Cross Effect

To evaluate the heteronuclear cross effect (hn-CE) DNP dynamics, we consider two microwave irradiated electron spins  $\mathbf{S}_{1,2}$  with the first electron spin interacting with a single nuclear spin  $\mathbf{I}$  of the  $^1\text{H}$  species and a single

nuclear spin  $\mathbf{J}$  of the  $^{19}\text{F}$  species. The effective Hamiltonian written in the microwave rotating frame has the form

$$\hat{H}_{\text{hnCE}} = \hat{H}_{\text{hnCE}}^0 + \hat{H}_{\text{hnCE}}^{\text{mw}} + \hat{H}_{\text{hnCE}}^{\text{en}} \quad (42)$$

where  $\hat{H}_{\text{hnCE}}^{\text{mw}}$  characterizes the microwave irradiation energy,  $\hat{H}_{\text{hnCE}}^{\text{en}}$  describes the semi-secular electron-nuclear interaction energy,  $\hat{H}_{\text{hnCE}}^0$  is built of electron and nuclear Zeeman interaction energy and the energy of the electron dipolar coupling. Specifically,

$$\begin{aligned} \hat{H}_{\text{hnCE}}^{\text{mw}} &= \frac{\omega_1}{2} \sum_{j=1}^2 \left( \hat{S}_{j+} + h.c. \right), \\ \hat{H}_{\text{hnCE}}^{\text{en}} &= \frac{1}{2} \left( B^{(H)} \hat{I}_+ + B^{(F)} \hat{J}_+ + h.c. \right) \hat{S}_{1z}, \\ \hat{H}_{\text{hnCE}}^0 &= \sum_{j=1}^2 \left( \Delta_j \hat{S}_{jz} \right) + \omega_H \hat{I}_z + \omega_F \hat{J}_z + \\ &+ D \left( 2S_{1z} \hat{S}_{2z} - \frac{1}{2} \hat{S}_{1+} \hat{S}_{2-} - \frac{1}{2} \hat{S}_{1-} \hat{S}_{2+} \right) \end{aligned} \quad (43)$$

with the microwave field strength  $\omega_1$ ,  $^1\text{H}$  and  $^{19}\text{F}$  electron-nuclear interaction strengths  $B^{(H)}, B^{(F)}$ , nuclear Larmor frequencies  $\omega_H, \omega_F$ , the offsets  $\Delta_{1,2}$  of the electron Larmor frequencies from the microwave frequency and the electron-electron interaction strength  $D$ .

For simplicity, we neglect the interactions  $\mathbf{S}_2 - \mathbf{I}$  and  $\mathbf{S}_2 - \mathbf{J}$  of the nuclei with the second electron and ignore the secular part of the  $\mathbf{S}_1 - \mathbf{I}$  and  $\mathbf{S}_1 - \mathbf{J}$  interactions, as the latter does not participate in the resonance condition (see below). We neglect also interactions between the nuclear spins assuming that spin  $\mathbf{I}$  of the  $^1\text{H}$  species belong to a close electron vicinity while spin  $\mathbf{J}$  of the  $^{19}\text{F}$  species is relatively remote from the electrons.

We assume that the difference  $\Delta_1 - \Delta_2$  between the electron frequency offsets is caused by the electron  $g$ -anisotropy and the secular part of the interaction between the electrons and nuclear spins.

The hn-CE resonance condition imposed on the effective offsets  $\Delta_{1,2}$  is formulated in terms of the projection of the Zeeman orders of the full Hamiltonian onto the subspace generated by the system of  $\mathbf{S}_{1,2}$  and  $\mathbf{I}, \mathbf{J}$  spins,

$$\begin{aligned} \hat{H}_Z &= \sum_{j=1}^2 \left( \Delta'_j \hat{S}_{jz} + \sum_k A_k^{(j)} \hat{I}_{kz}^{(j)} \hat{S}_{jz} \right) + \\ &+ \omega_H \hat{I}_z + \omega_F \hat{J}_z + A^{(H)} \hat{I}_z \hat{S}_{1z} + A^{(F)} \hat{J}_z \hat{S}_{1z}. \end{aligned}$$

Here  $A^{(H)}, A^{(F)}$  are the secular strengths of the  $\mathbf{S}_1 - \mathbf{I}, \mathbf{S}_1 - \mathbf{J}$  coupling,  $A_k^{(j)}$  are the secular strengths of the coupling between the electrons and nuclear spins  $\mathbf{I}_k^{(j)}$  other than  $\mathbf{I}, \mathbf{J}$ . We use also the electron frequency offsets  $\Delta'_{1,2}$  before taking into account the hyperfine coupling.

The resonance condition relevant to hn-CE in the  $^1\text{H} - ^{19}\text{F}$  require that either the  $|\alpha_{1e}\beta_{2e}\alpha_H\beta_F\rangle$

and  $|\beta_{1e}\alpha_{2e}\beta_H\alpha_F\rangle$  states or the  $|\alpha_{1e}\beta_{2e}\beta_H\alpha_F\rangle$  and  $|\alpha_{1e}\beta_{2e}\beta_H\alpha_F\rangle$  states are degenerate. In other words, one of the following two conditions is satisfied

$$\Delta_1 - \Delta_2 = \omega_2 - \omega_1, \quad \Delta_1 - \Delta_2 = \omega_1 - \omega_2 \quad (44)$$

where

$$\Delta_j = \Delta'_j + \sum_k A_k^{(j)} \hat{I}_{kz}^{(j)}, \quad j = 1, 2,$$

are the effective electron frequency offsets that depend on orientations of the ‘‘external’’ nuclear spins  $\mathbf{I}_k^{(j)}$ . Notably, the secular part of the  $\mathbf{S}_1 - \mathbf{I}$  or  $\mathbf{S}_1 - \mathbf{J}$  hyperfine interaction does not affect the resonance conditions.

### Density Matrix Simulations

In simulations, we use the master equation

$$\frac{d}{dt} \hat{\rho} = -i[\hat{H}_{\text{eff}}, \hat{\rho}] + \hat{\mathcal{D}}\hat{\rho},$$

where  $\hat{H}_{\text{eff}}$  is an effective Hamiltonian describing either hn-TM, SE or CE, is given by Eqs. (40,41,42,43) and the standard Lindbladian relaxation model is used that describes single-spin Markovian jumps,

$$\begin{aligned} \hat{\mathcal{D}}\hat{\rho} &= \sum_{j=1}^2 \left[ \Gamma_{1+} \mathcal{L}(\hat{S}_{j+}) + \Gamma_{1-} \mathcal{L}(\hat{S}_{j-}) + \Gamma_2 \mathcal{L}(\hat{S}_{jz}) \right] + \\ &+ \gamma_+^{(H)} \mathcal{L}(\hat{I}_+) + \gamma_{1-}^{(H)} \mathcal{L}(\hat{I}_-) + \gamma_2^{(H)} \mathcal{L}(\hat{I}_z) + \\ &+ \gamma_+^{(F)} \mathcal{L}(\hat{J}_+) + \gamma_{1-}^{(F)} \mathcal{L}(\hat{J}_-) + \gamma_2^{(F)} \mathcal{L}(\hat{J}_z) \\ \Gamma_{1\pm} &= \frac{1 \mp p_e}{2} R_1, \quad \Gamma_2 = 2R_2, \\ \gamma_{1\pm}^{(H)} &= \frac{1 \mp p_n^{(H)}}{2} r_1^{(H)}, \quad \gamma_{1\pm}^{(F)} = \frac{1 \mp p_n^{(F)}}{2} r_1^{(F)}, \\ \gamma_2^{(H)} &= 2r_2^{(H)}, \quad \gamma_2^{(F)} = 2r_2^{(F)}. \end{aligned}$$

Here  $p_e, p_n^{(H)}$  and  $p_n^{(F)}$  are the thermal polarizations of the electron and  $^1\text{H}$  or  $^{19}\text{F}$  spins,  $R_{1,2}, r_{1,2}^{(H)}, r_{1,2}^{(F)}$  are the electron and nuclear longitudinal and transverse relaxation rates and we use the notation

$$\mathcal{L}(\hat{X})\rho \equiv \hat{X}\hat{\rho}\hat{X}^\dagger - \frac{1}{2} \left( \hat{X}^\dagger \hat{X}\hat{\rho} + \hat{\rho}\hat{X}^\dagger \hat{X} \right).$$

Numerical solution of the master equation is used to produce a macroscopic sweep DNP spectrum for SE and hn-TM. To estimate the macroscopic sweep DNP spectrum for CE, the system is tuned to one of the resonances given by Eq. (44)

$$\Delta_2 = \Delta_1 \pm \delta, \quad \delta \equiv \omega_1 - \omega_2,$$

the first electron frequency offset  $\Delta_1$  is swept and then the convolution is taken of the resulting nuclear polarizations  $p_{\pm}^{(j)}(\Delta_1)$  with the shape  $g(\omega)$  of the ESR line

$$\begin{aligned} \bar{p}^{(j)}(\omega) = \int_{-\infty}^{+\infty} g(\omega + \Delta_1) & \left[ g(\omega + \Delta_1 + \delta) p_{+}^{(j)}(\Delta_1) + \right. \\ & \left. + g(\omega + \Delta_1 - \delta) p_{-}^{(j)}(\Delta_1) \right] d\Delta_1, \end{aligned} \quad (45)$$

where  $\omega$  is the microwave frequency.

---

[1] I. Gromov, V.Krymov, P. Manikandan, D. Arieli, D. Goldfarb, *J. Magn. Reson.*, 1999, **139** , 817.

- [2] I. Solomon, *Phys. Rev.* 1955, **99** , 559565.  
 [3] W. de Boer, *J. Low Temp. Phys.* 1976, **22** , 185212.  
 [4] L. Lumata, Z. Kovacs, A.D. Sherry, C. Malloy, S. Hill, J. Van Tol, L. Yu, L. Song, M.E. Merritt, *Phys. Chem. Chem. Phys.* 2013, **15** , 98009807.  
 [5] U. Haerberlen and J.S. Waugh, *Phys. Rev.*, 1968, **175**, 453-467.  
 [6] M.Leskes, P.K. Mahdu, S. Vega, *Prog. Nucl. Magn. Reson. Spec.*, 2010, **57**, 345-380.  
 [7] A. Karabanov, A. van der Drift, I. Kuprov, L. J. Edwards, W. Köckenberger, *Phys. Chem. Chem. Phys.*, 2012, **14**, 2658-2668.  
 [8] A. Karabanov, G. Kwiatkowski, W. Köckenberger, *Appl. Magn. Reson.*, 2012, **43**, 43-58.  
 [9] M. Bennati, C.T. Farrar, J. A. Bryant, S.J. Inati, V. Weis, G.J. Gerfen, P. Riggs-Gelasco, J. Stubbe, R.G. Griffin, *J. Magn. Reson.*, 1999, **138**, 232-243.